Diffusion Tensor Digital Phantom for Crossing Fibres Detection

Fahimeh Dargi
Department of medical physics and Biomedical engineering, Tehran University of Medical Science
dargi@razi.tums.ac.ir

Mohammad Ali Oghabian
Department of medical physics and Biomedical engineering, Tehran University of Medical Science
oghabian@sina.tums.ac.ir

Alireza Ahmadian
Department of medical physics and Biomedical engineering, Tehran University of Medical Science
ahmadian@sina.tums.ac.ir

Hamid Soltanian Zadeh
Department of Electrical and Computer Engineering, University of Tehran
hszadeh@ut.ac.ir

Mojtaba Zarei
Department of Clinical Neurology, University of Oxford
mojtaba@fmrib.ox.ac.uk

Abstract: *White matter tractogarphy is a non-invasive method for reconstructing three dimensional fibre pathways of the brain. Several fibre tracking algorithms have been proposed for this purpose. To evaluate and compare these algorithms, it is required to use synthetic datasets for which the simulated pathways are known to the user. This paper describes an algorithm designed in Matlab to simulate a diffusion tensor digital phantom for evaluating white matter fibre tractography algorithms and assessing their ability to detect fibre crossing. This digital phantom allows quantitative assessment of the robustness of fibre tracking algorithms by varying the thickness, the angles between crossing fibres, the Fractional Anisotropy (FA) value of synthetic paths, and background.*

Keywords: *Diffusion Tensor Imaging (DTI), fibre tractography, digital phantom, simulation, evaluation, crossing fibres.*

1   Introduction

Diffusion Tensor Imaging (DTI) is a non-invasive tool to measure random motion of water molecules called diffusion or "Brownian motion". In isotropic environments, the molecules move equally in all directions but diffusion is restricted in anisotropic regions. Brain white matter is an anisotropic tissue containing axons of neurons. The myelin sheet of axons restricts motion of the water molecules. In white matter, groups of axons bundle together and construct tracts. Diffusion in the direction parallel to these tracts is at least twice faster than in the perpendicular directions [3]. One of the most important applications of diffusion tensor imaging is white matter tractography, which non-invasively reconstructs a three dimensional trajectory of the white matter fibre pathways.

Diffusion properties of the neural pathways can be obtained by this imaging technique, where a symmetric 2nd-order tensor is assigned to each image voxel. The principal eigenvalue of each voxel's tensor represents the direction of white matter fibre bundles. Measures of the diffusion tensor can be used to investigate brain white matter pathways development and help for neurosurgical planning. This derived information can be used to assess neurologic diseases like Multiple Sclerosis, Schizophrenia, Alzheimer, and Epilepsy [5].

In recent years, several tractography algorithms have been proposed to reconstruct the

neural pathways and to find white matter tracts connecting different brain regions. However, due to the limitations of the diffusion tensor imaging, e.g., the partial volume effect, some of these tractography algorithms are unable to detect correct pathways in crossing and branching fibres. In crossing fibres, the voxels containing multiple fibre bundles with different orientations, do not represent the main diffusion direction. A reliable algorithm is the one that correctly find the fibres in these regions.

In order to evaluate the ability and robustness of different white matter tractography algorithms, it is recommended to use simulated DTI data, in which its synthetic tracts are known.

Basser et al. [7] generated a two dimensional diffusion tensor dataset containing several rings with different radius of curvature. Two three dimensional simulated dataset were generated by Tournier et al. [8]. One of them had a half cylinder shape and another one was a fibre that reconstructed a semicircular path. Ning Kang et al. [9] simulated three single-turn helical fibre bundles in a three dimensional volume. They also simulated two straight line fibre bundles which crossed each other at the right angle. Staempli et al. [10] generated an artificial data which is consisted of two intersecting cylinders to assess the ability of Advanced Fast Marching algorithm in tracking crossing fibres. Some virtually three dimensional phantoms were reconstructed in kissing and twisting [11] and helical [12,13] shape fibres. Leemans et al. [14] simulated a synthetic DT-MRI phantom that reconstructed the physical properties of a fibre pathway by the Gaussian and saturated model.

This paper describes an algorithm to simulate a synthetic diffusion tensor dataset as a testing framework for evaluating the ability of white matter fibre tractography algorithms to detect fibre crossing. Using this dataset one can assess the robustness of any fibre tracking algorithm by varying the thickness and angles between crossing fibres. The number of gradient directions and the factional anisotropy of the fibre pathways and surrounding regions can be varied to obtain different simulated diffusion weighted images. Different levels of noise can be added to the diffusion weighted images for quantitative evaluation of specified algorithm's noise sensitivity. By generating a sample synthetic dataset with constant parameters, one can compare several tractography algorithms quantitatively.

2 Background Theory

To compute diffusion tensor, a raw data source, i.e., diffusion weighted images are used. These images are sensitive to displacement of proton molecules along the axis of applied diffusion gradient in Stejskal-Tanner Imaging sequence [1]. The amount of signal loss by gradient application is given by the Stejskal-Tanner equation [1,2]:

$$S = S_0 e^{-\gamma^2 \delta^2 [\Delta - \delta/3]|G|^2 \, g^T D g} \qquad (1)$$

where S_0 is the signal intensity without diffusion weighting and S is the signal intensity with applying diffusion gradient, γ is the Larmor constant, δ is the gradient pulse width, Δ is the time between gradient pulses, $|G|$ is the strength of the gradient pulses, g is the applied gradient table in three main axis directions and D is the diffusion constant.

By introducing the b-value, the above equation can be written as;

$$S = S_0 e^{-b g^T D g} \qquad (2)$$

where

$$b = \gamma^2 \delta^2 [\Delta - \delta/3]|G|^2 . \qquad (3)$$

In isotropic environment, the diffusion constant is scalar, but in anisotropic regions a 2nd-order tensor model represents the diffusion. This tensor is a 3x3 symmetric matrix, with 6 independent elements:

$$D = \begin{bmatrix} D_{xx} & D_{xy} & D_{xz} \\ D_{xy} & D_{yy} & D_{yz} \\ D_{xz} & D_{yz} & D_{zz} \end{bmatrix} \qquad (4)$$

This tensor has three eigenvalues and three corresponding eigenvectors. As shown in Figure 1(a), the tensor has equal eigenvalues in isotropic regions, whereas in anisotropic environment the eigenvalues are not equal and the eigenvector of the maximum eigenvalue is the principal eigenvector, which determines the preferred pathway direction in each voxel. By tracking the principal eigenvalues of the voxels, the fibres can be extracted from the diffusion weighted images. The anisotropic tensor shape with its eigenvalues is represented in Figure 1 (b).
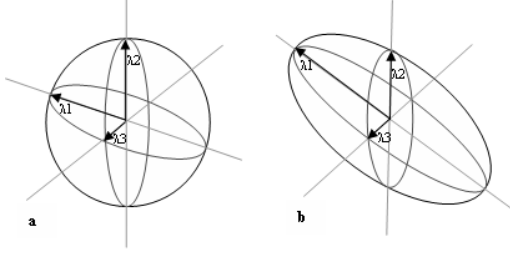
Figure 1: Tensor shapes in (a) isotropic and (b) anisotropic regions.

By providing non-diffusion image, b value, diffusion weighted images, and gradient table, the tensor elements of each voxel can be calculated using:

$$g^T D g = -\frac{1}{b}\ln(\frac{S}{S_0}) \qquad (5)$$

where S is the voxel intensity of each diffusion weighted images and S_0 is the voxel intensity of non-diffusion image. By solving Equation (5), six unknown tensor's elements (i.e., D_{xx}, D_{yy}, D_{zz}, D_{xy}, D_{xz}, D_{yz}) are determined:

$$\begin{bmatrix} g_x & g_y & g_z \end{bmatrix} \begin{bmatrix} D_{xx} & D_{xy} & D_{xz} \\ D_{xy} & D_{yy} & D_{yz} \\ D_{xz} & D_{yz} & D_{zz} \end{bmatrix} \begin{bmatrix} g_x \\ g_y \\ g_z \end{bmatrix} = \begin{bmatrix} \frac{1}{b}\ln(\frac{s_0}{s}) \\ \frac{1}{b}\ln(\frac{s_0}{s}) \\ \frac{1}{b}\ln(\frac{s_0}{s}) \end{bmatrix} \qquad (6)$$

$$\begin{bmatrix} g_x^2 & g_y^2 & g_z^2 & 2g_x g_y & 2g_x g_z & 2g_y g_z \end{bmatrix} \begin{bmatrix} D_{xx} \\ D_{yy} \\ D_{zz} \\ D_{xy} \\ D_{xz} \\ D_{yz} \end{bmatrix} = \begin{bmatrix} \frac{1}{b}\ln(\frac{s_0}{s}) \\ \frac{1}{b}\ln(\frac{s_0}{s}) \\ \frac{1}{b}\ln(\frac{s_0}{s}) \end{bmatrix} \qquad (7)$$

The eigenvectors and eigenvalues of each voxel can be calculated from its tensor. By applying the rotation operator on the eigenvector's matrix, one can obtain the rotated tensor's eigenvector around z axis and y axis.

Using this rotated eigenvectors and the corresponding eigenvalues, its symmetric tensor can be calculated:

$$Rotated\ D = V^{-1} E\ V \qquad (8)$$

where V is the rotated eigenvector's and E is the eigenvalue's matrix.

Fractional Anisotropy (FA) of each voxel is computed from the following equation:

$$FA = \frac{\sqrt{3[(\lambda_1 - \langle\lambda\rangle)^2 + (\lambda_2 - \langle\lambda\rangle)^2 + (\lambda_3 - \langle\lambda\rangle)^2]}}{\sqrt{2(\lambda_1^2 + \lambda_2^2 + \lambda_3^2)}} \qquad (9)$$

where λ_1, λ_2, λ_3 are three tensor's eigenvalues and the mean diffusivity is determined by:

$$\langle\lambda\rangle = \frac{\lambda_1 + \lambda_2 + \lambda_3}{3} . \qquad (10)$$

The FA value is normalized between zero and one. The FA value of isotropic regions like grey matter is less than 0.25 and for anisotropic regions like white matter is greater than 0.25 [16].

3   Methods

For simulating DTI dataset, and generating a diffusion tensor digital phantom, we developed an algorithm and designed a graphical user interface (GUI) in MATLAB environment. The simulated diffusion weighted images can also be constructed from this DTI dataset. Figure 2 shows a block diagram of the proposed algorithm.
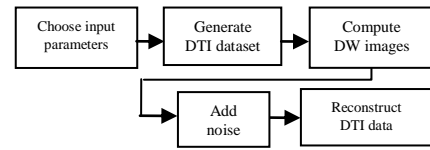

Figure 2: Block diagram of the algorithm for generating diffusion tensor dig ital phantom

In the first step of the algorithm, the input parameters for generating the synthetic paths can be entered by the user. These synthetic fibre bundles are multiple circular paths with fibre crossings at different angles. In the designed GUI, the user can select the number of circular paths as well as their thickness and radius. Tensor elements of fibres are obtained from real DTI dataset with FA value greater than 0.25. The FA value of background voxels can also be set less than 0.25. For generating each circular path, the tensor of the first point can be defined by the selected FA value. Eigenvectors and eigenvalues of this tensor are calculated. Eigenvectors of next voxels in the circular fibre can be obtained from multiplying the rotation matrix by the eigrenvector's matrix. Thus, the rotated symmetric tensor can be computed by the eigenvectors and the corresponding eigenvalues.

To add a crossing fibre, its location is chosen by selecting the number of crossing fibres, e.g., for 8 crossings, the circular paths is divided to eight parts and the crossing fibre's locations are selected. The tensor of this location is obtained, and the required crossing fibres are constructed with the ordered angle, thickness, and FA value. Figure 3 schematically shows a circular path with 6 crossing fibres, where the principal direction of each voxel's tensor represents by color coding in all three directions in space as shown in the upper right corner of the figure. The input parameters of crossing fibres, can be entered by user. In the represented synthetic dataset the angles are

defined, $90°$, $75°$, $60°$, $45°$, $30°$, $15°$ and then the crossing fibres are constructed, respectively in the counter clockwise direction. The suggested seed point for implementing tractography is also shown in this figure. For example, a tractography method may detect all crossing angles greater than $45°$ but not less than $30°$.
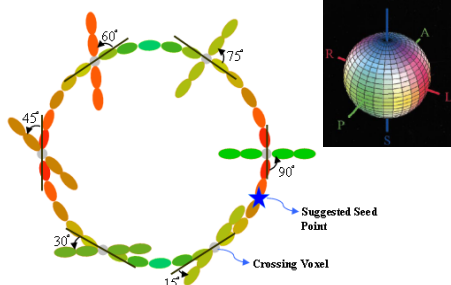

Figure 3: A circular path with 6 crossing fibers. Colour coding scheme is shown in upper right of the figure.

After generating the simulated DTI dataset, the simulated diffusion weighted images can be constructed. In this step, by selecting the gradient directions, the same number of diffusion weighted images is obtained from the simulated DTI dataset using Equation (2). Gaussian noise with different standard deviations [6] can be added to the diffusion weighted images to prepare the desired signal-to-noise ratio (SNR) for evaluation of the noise sensitivity of algorithms. Using this simulated diffusion weighted images and the corresponding gradient table, the DTI dataset can be reconstructed by Equation (3).

For generating a testing DTI data with real background and simulated fibre pathways, tensors of the simulated pathways can replace the corresponding voxel's tensors in real DTI data. Figure 4 shows the block diagram of the algorithm for generating this synthetic data.
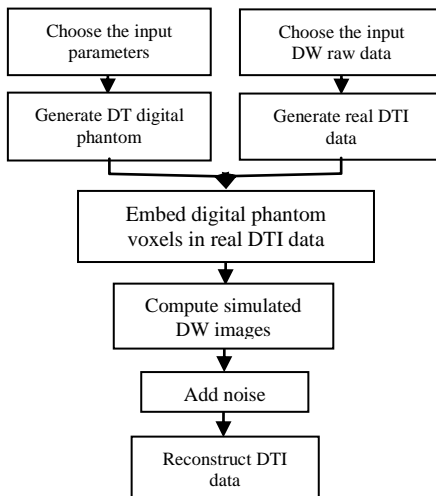

Figure 4: Block diagram of the algorithm for generating synthetic DTI data with real background.

To implement this, first the real DTI data is computed using raw dataset by Equation (5), and in the other hand the synthetic fibres is generated. Then the synthetic fibre's voxels are embedded in the real DTI data. Using this artificial data, one can prepare the simulated diffusion weighted images. By adding noise to these images, the noisy simulated DTI dataset can be generated.

For generating more realistic synthetic fibre, we extracted a tract from a human brain's DTI data. This tract is thinned to one voxel thickness. Tensors with the selected FA value are assigned to its voxels. By the way for increasing the thickness of this fibre, a binary kernel consisted of a white sphere within a black background is convolved to this tract. The diameter of this sphere sets the thickness of the fibre.

In order to constructing a realistic crossing fibre, we rotated this pathway with the arbitrary angle and then added it to the first one. All the tensors in the crossing region are sum of the tensors of paths which crossed each other. Figure 5 schematically shows a realistic fibre crossing.
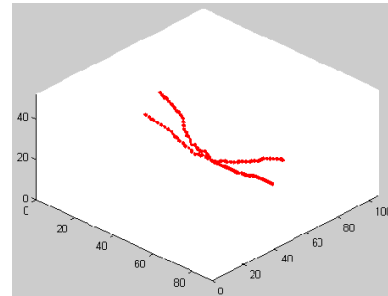

Figure 5: A realistic fibre crossing with $30°$.

4   Results

The designed user interface is able to construct the simulated DTI data and display the corresponding diffusion weighted images. This GUI prepares three types of DTI datasets:

1. Real data
2. Simulated data
3. Real plus simulated data

Figure 6 shows the appearance of this GUI. By selecting each of the above dataset, the required parameters can be acquired from the user and then the dataset will be reconstructed. The diffusion weighted images will be shown in the image viewer part. These images can be saved in dicom format for easy conversion and loading in any fibre tractography and DTI analyzing software.
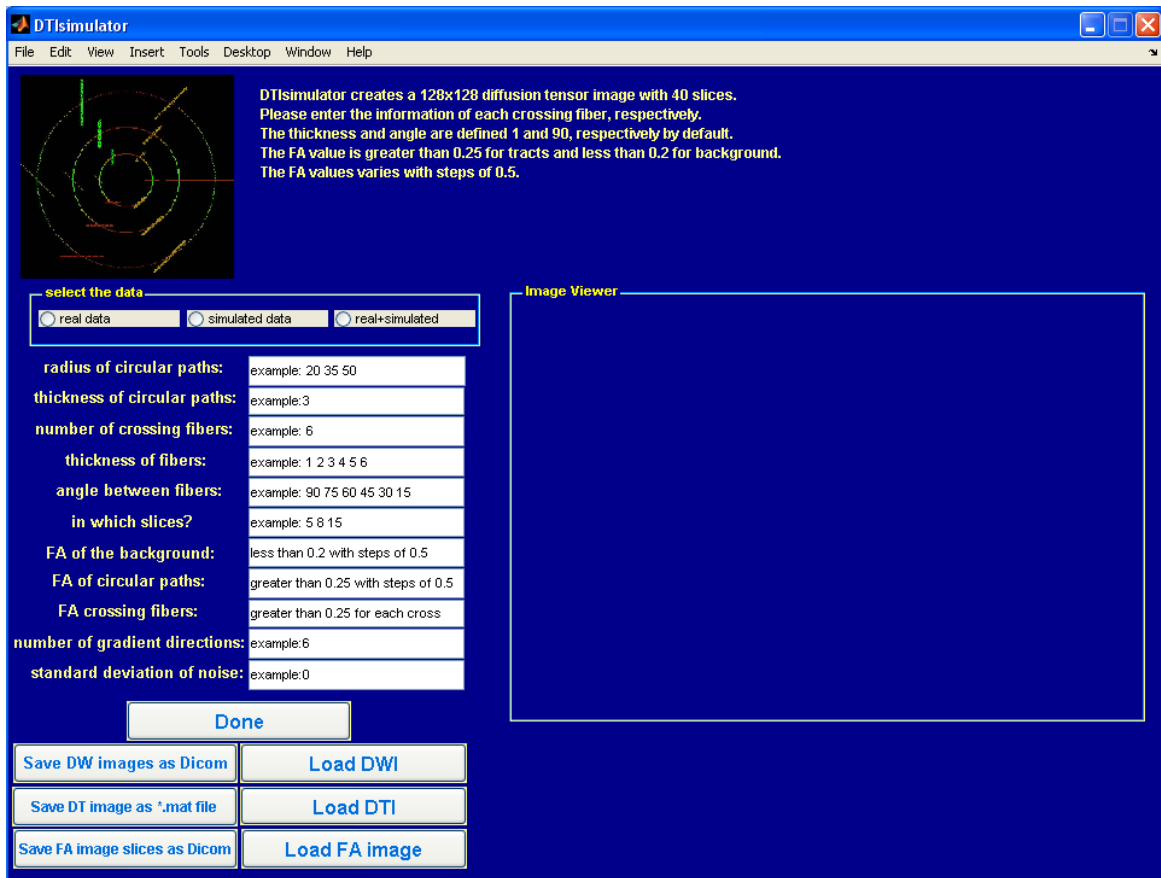
Figure 6:   A view of the developed graphical user interface

4.1   Real data

By selecting the real data in GUI, a real DWI data with the chosen number of gradient direction is loaded and the DTI data is generated from this dataset using Equation (5). Gaussian noise with desired standard deviation can be added to the diffusion weighted images, thus the noisy DTI data can be reconstructed from them. Figure 7 shows real diffusion weighted images which are loaded in Image Viewer of the GUI. This real raw data is loaded in FSL [17] and the color coded DTI dataset and the principal eigenvectors are shown in Figures 8 (a) and (b), respectively.
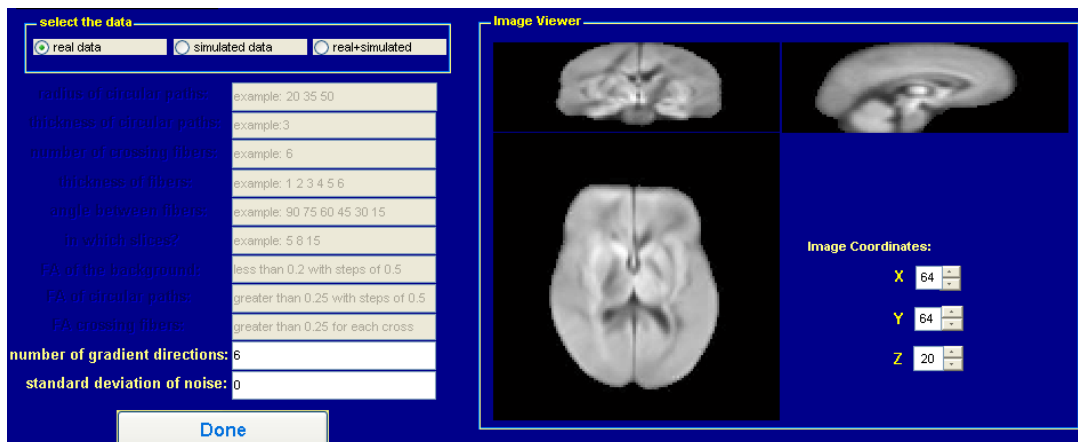

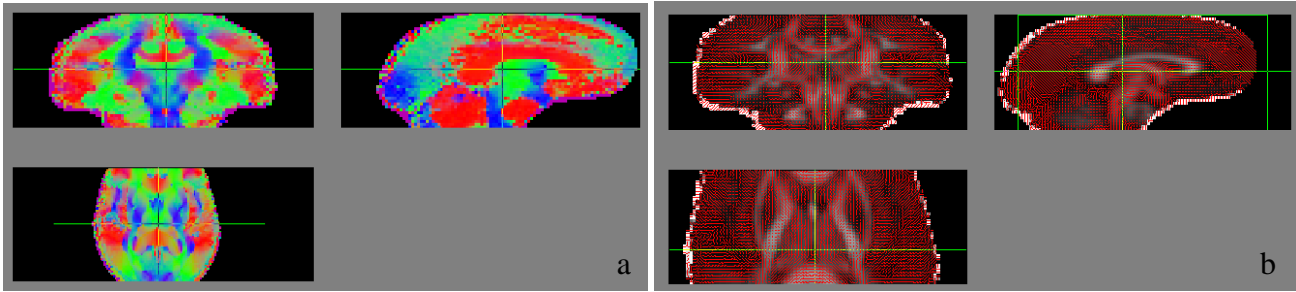Figure 7: Real diffusion weighted image with 6 gradient directions and without noise.

Figure 8: (a) View of color coded DTI data, and (b) View of principal eigenvectors in the FSLview .

4.2 Simulated data

Once the simulated data is selected, the synthetic circular fibre pathways can be generated by user's input parameters and for any number of crossing fibres, the crossing's places are determined and the tensor of these voxels are selected. The parameters of each crossing (e.g. the FA value, thickness, and angles) are entered and the crossing fibres can be generated.

This section follows the algorithm described schematically in Figure 2. In this step, we have a synthetic DTI data and for the next stage diffusion weighted images are computed from this DTI data using Equation (2). The number of acquired diffusion weighted images is determined by the number of gradient directions. Gaussian noise can be added to these diffusion weighted images. Using diffusion weighted images and gradient direction the DTI data can be reconstructed by Equation (5).

By the defined input parameters shown in Figure 9(a), a three dimensional digital phantom can be constructed and the simulated diffusion weighted images are generated in dicom format. These dicom images are converted in NIFTI format and loaded in FSL. A view of the FSL results of colour coded DTI data and diffusion fitting by principal eigenvectors are shown respectively in Figures 9(b) and (c). As this result represents the eigenvectors are correctly matched to their paths.
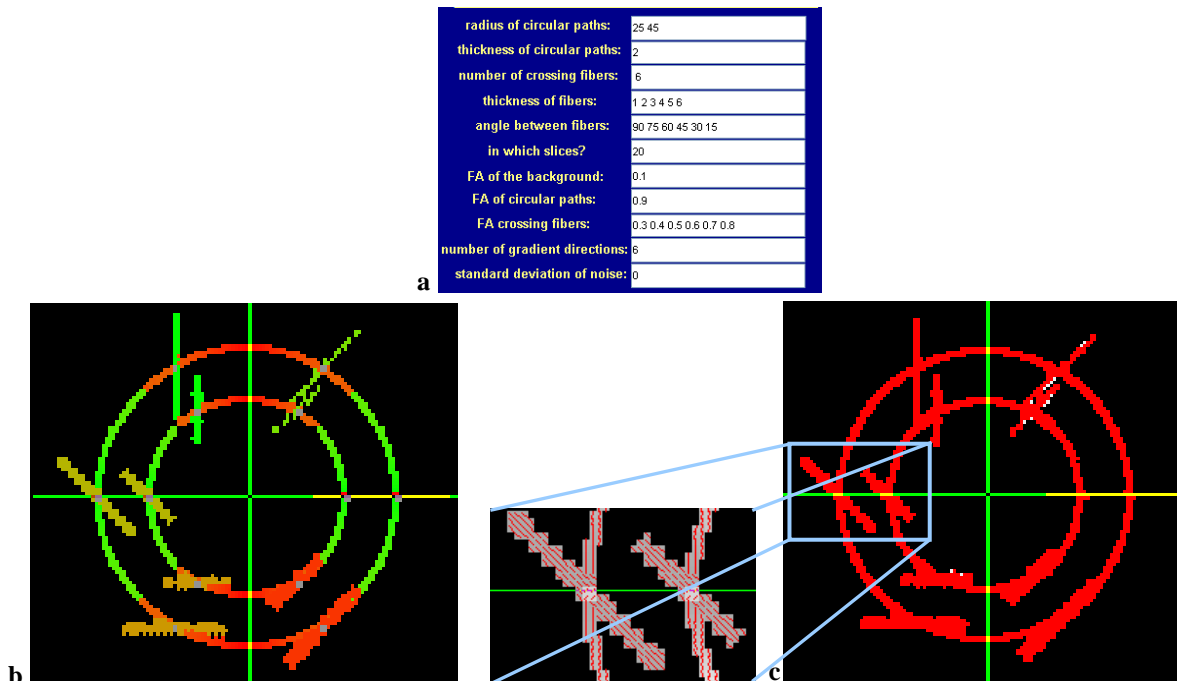

Figure 9: (a) Input parameters for creating a 3D diffusion tensor digital phantom. (b) View of colour coded DTI data, and (c) View of principal eigenvectors in FSLview.
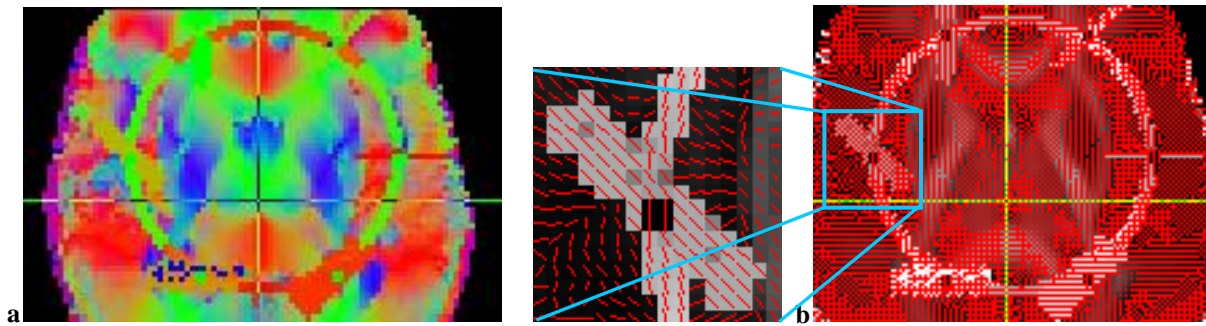
Figure 10: 3D simulated tracts that are embedded in real data which is shown in Figure 7. The synthetic tracts can be seen in (a) colour coded DTI data. (b) View of principal eigenvectors in FSLview.

4.3 Real plus simulated data

By choosing real+simulated data in the designed GUI, the algorithm illustrated in the block diagram of Figure 5 is executed. The DTI data is generated from real diffusion weighted images and the simulated tensors are inserted in the corresponding locations in the real data. The simulated diffusion weighted images with their gradient table are loaded in FSL. The result of this part is shown in Figure 9. As shown in this figure, the simulated DTI dataset has a real background that the artificial fibre pathways are embedded in it.

Like the previous sections, noise can be added to the diffusion weighted data and noisy DTI dataset can be reconstructed. The resulting data is used for testing the noise sensitivity of the algorithms.

Fibre tracking results

We use probabilistic tractography algorithm [18] and fast marching algorithm [19] for implementing fibre tracking on this simulated data.

As shown in figure 11(a) fast marching algorithm detects all the crossing fibres, whereas probabilistic algorithm is unable to detect the crossing region. Figure 11(b) illustrates that the tracking is cut in crossing regions and unable to continue the pathway.
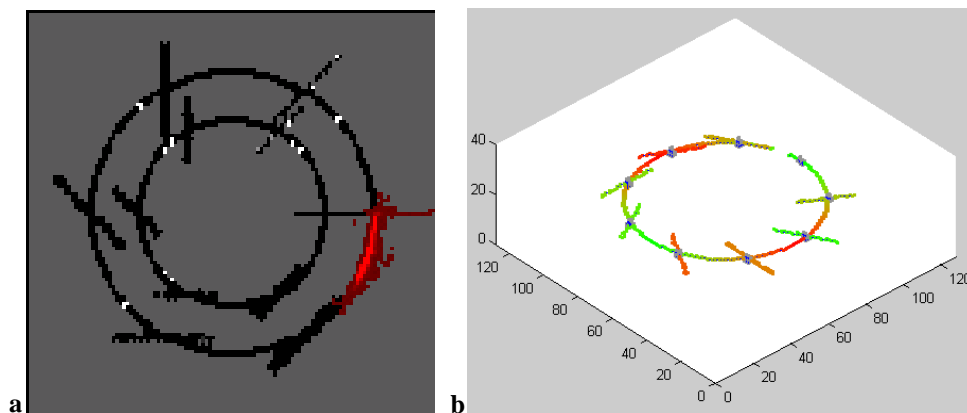

Figure 11: Result of fiber tracking using (a) Probabilistic tractography algorithm, (b) Fast Marching algorithm.

5   Conclusion

This proposed simulated dataset can be used as a quantitative testing framework for evaluating the robustness, noise sensitivity, and performance of DTI fibre tractography algorithms. Using this simulated dataset, we assessed how a true crossing can be detected in different conditions such as background noise, different FA value of fibres and background environment, crossing angle, and thickness.

Using real diffusion weighted data, for the background of the image, the synthetic fibres are embedded in the real environment, thus a dataset with real background can be constructed.

The resulting simulated diffusion weighted images are saved in a dicom format so that they can be used in different fibre tracking software.

After converting the simulated raw dataset to NIFTI format, we tested this 3D digital phantom in FSL. As shown in Figure 9 (c) and Figure 10 (b), the principal eigenvectors are correctly fitted to this data.

References

[1] Susumu Mori, Peter B. Barker, "Diffusion Magnetic Resonance Imaging: Its Principal and Applications", The Anatomical Record, vol. 257, pp. 102-109, 1999.

[2] C.-F.Westin, S.E. Maier, B. Khidhir et al. , "Image Processing of Diffusion Tensor Magnetic Resonance Imaging", In Proceeding of Second Int. Conf on Medical Image Computing and Computer-assisted Interventions, pp. 441-452, 1999.

[3] Roland Bammer, Burak Acar, Micheal E. Moseley, "In Vivo MR Tractography Using Diffusion Imaging", European Journal of Radiology, vol.45, pp. 223-234, 2003.

[4] Denis le Bihan, Jean-Francois Mangin, Cyril Poupon, "Diffusion Tensor Imaging: Concepts and Applications", Journal of Magnetic Resonance Imaging, vol. 13, pp. 534-546, 2001.

[5] Elias R.Melhem, Susumu Mori, Govind Mukundan, "Diffusion Tensor MR Imaging of the Brain and White Matter Tractography", American Journal of Radiology, vol. 178, pp. 3-16, 2002.

[6] Peter B. Kingsley, "Introduction to Diffusion Tensor Imaging Mathematics: Part III. Tensor Calculation, Noise, Simulation, and Optimization", Published online in Wiley Interscience, Concepts Magnetic Resonance, part A, pp. 155-179, 2006.

[7] Peter J. Basser, Sinisa Pajevic, Carlo Pierpaoli, "In Vivo Fibre Tractography Using DT-MRI Data", Magnetic Resonance in Medicine, vol. 44, pp.625-632, 2000.

[8] J. D. Tournier, F. Calamante, M.D.King, "Limitations and Requirements of Diffusion Tensor Fibre Tracking: An Assessment Using Simulations", Magnetic Resonance in Medicine, 2002, vol. 47, pp. 701-708.

[9] Ning Kang, Jun Zhang, Eric S. Carlson, "White Matter Fibre Tractography Via Anisotropic Diffusion Simulation in the Human Brain", IEEE Transactions on Medical Imaging, vol. 24, No.9, pp.1127-1137, 2005.

[10] P.Staempfli, T. Jaermann, G. Crelier, "Resolving Fibre Crossing Using Advanced Fast Marching Tractography Based on Diffusion Tensor Imaging", NeuroImage, vol. 30, pp. 110-120, 2006.

[11] urak Acar, Rolan Bammer, Michael Moseley, "Comparative Assessment of DT-MRI Fibre Tractography Algorithms". Proceedings of ISMRM, pp.2164, July 2003.

[12] Orjan Bergmann, Arvid Lundervold, Trond Steihaug, "Generating a Synthetic Diffusion Tensor Dataset", Proceeding of the 18th IEEE Symposium on Computer-Based Medical Systems, 2005.

[13] Alexander J. Taylor, "Diffusion Tensor Imaging: Evaluation of Tractography Algorithm Performance Using Ground Truth Phantoms", Master Thesis, May 2004.

[14] A. Leemans, J. Sijbers, M. Verhoye, "Mathematical Framework for Simulating Diffusion Tensor MR Neural Fibre Bundles", Magnetic Resonance in Medicine, vol. 53, pp. 944-953, 2005.

[15] Papadakis, D.Xing, "A comparative study of Acquisition Schemes for Diffusion Tensor Imaging Using MRI", Journal of Magnetic Resonance, vol. 137, pp. 67-82, 1999.

[16] Pierpaoli, P.Jezzard,"Diffusion Tensor MR Imaging of the Human Brain", Radiology, vol.201, No. 3, pp. 637-648, 1996.

[17] www.fmrib.ox.ac.uk/fsl/

[18] Geoffrey J. M. Parker, Claudia A. M. Wheeler-Kingshott, and Gareth J. Barker," Estimating Distributed Anatomical Connectivity Using Fast Marching Methods and Diffusion Tensor Imaging", IEEE TRANSACTIONS ON MEDICAL IMAGING, VOL. 21, NO. 5, MAY 2002.